



Cite this: *RSC Adv.*, 2025, **15**, 48216

## Antiviral and virucidal activities against SARS-CoV-2 and antibacterial properties of bile acids and their salts with naturally occurring organic cations of L-carnitine, creatinine, and choline

Chavalit Varongkriengkrai,<sup>a</sup> Nopporn Chutiwitoonchai,<sup>ID \*b</sup> Nontaphat Leerach,<sup>c</sup> Sanya Sureram,<sup>d</sup> Tam Pooprasert,<sup>a</sup> Thammarat Aree,<sup>ID e</sup> Sakda Khoomrung,<sup>fghi</sup> Chulabhorn Mahidol,<sup>d</sup> Somsak Ruchirawat<sup>adj</sup> and Prasat Kittakoop <sup>ID \*adj</sup>

Bile acids have many roles in biological systems, and they have received great attention recently. Bile from a cow, known as gall, together with garlic, wine, and leeks, is used in the traditional medicine recipe of Bald's Leechbook, a thousand-year-old Anglo-Saxon formula for the treatment of infected eyelash follicles. Different aspects of previous works on bile acids have been reported, and this work adds antiviral, virucidal, and antibacterial properties of bile acids and their salts against SARS-CoV-2. Four bile acids, lithocholic acid (LCA, 1), deoxycholic acid (DCA, 5), ursodeoxycholic acid (UDCA, 9), and chenodeoxycholic acid (CDCA, 13), were used to form salts with L-carnitine [X], creatinine [Y], and choline [Z], which are naturally occurring compounds. Bile acids and their salts were evaluated for antiviral and virucidal activities against SARS-CoV-2 as well as for their antibacterial properties. Among the bile acids tested, LCA (1) was found to display virucidal activity against SARS-CoV-2 with an EC<sub>50</sub> of 9.69 µg mL<sup>-1</sup> and a selectivity index (SI) of >5.16. However, its salts, [LCA][X] (2), [LCA][Y] (3), and [LCA][Z] (4), were 1.31–3.27 times less active than the bile acid LCA (1), indicating that salt forms of this bile acid did not have improved virucidal activity. Bile acids DCA (5), UDCA (9), and CDCA (13) exhibited antibacterial activity against Gram-positive bacteria (*Bacillus cereus*, *Staphylococcus aureus*, *Staphylococcus epidermidis*, and *Enterococcus faecalis*) and against a Gram-negative bacterium (*Escherichia coli*). Cholinium salts of these bile acids exhibited enhanced antibacterial activity; for example, 41.4–41.5% antibacterial improvement was observed for the [DCA][Z] (8) salt when compared with its corresponding bile acid DCA (5). This work provides evidence that certain salts of bile acids have improved antibacterial activity, but they do not enhance antiviral properties.

Received 16th October 2025  
Accepted 20th November 2025

DOI: 10.1039/d5ra07917a  
[rsc.li/rsc-advances](http://rsc.li/rsc-advances)

## 1 Introduction

COVID-19, an illness resulting from SARS-CoV-2 virus infection, is an ongoing global health crisis transmitted through close personal contact.<sup>1</sup> Since its initial outbreak in December 2019, it has significantly affected the world in many aspects. As of April

2025, COVID-19 has resulted in over 7 million deaths globally<sup>2</sup> and has triggered consequences across diverse sectors, including the physical and mental health, global economy, tourism, education systems, and environment.<sup>3–5</sup> Despite the availability of COVID-19 vaccines that have shown effectiveness in reducing both incidence and severity of the disease,<sup>6,7</sup> they do not offer complete protection against the infection.

<sup>a</sup>Chulabhorn Graduate Institute, Program in Chemical Sciences, Laksi, Bangkok 10210, Thailand

<sup>b</sup>National Center for Genetic Engineering and Biotechnology (BIOTEC), National Science and Technology Development Agency (NSTDA), 113 Thailand Science Park, Phahonyothin Rd., Pathumthani 12120, Thailand. E-mail: [nopporn.chu@biotec.or.th](mailto:nopporn.chu@biotec.or.th)

<sup>c</sup>Princess Srisavangavadhana Faculty of Medicine, Chulabhorn Royal Academy, Bangkok, 10210, Thailand

<sup>d</sup>Chulabhorn Research Institute, Kamphaeng Phet 6, Talat Bang Khen, Lak Si, Bangkok, 10210, Thailand. E-mail: [prasat@cri.or.th](mailto:prasat@cri.or.th)

<sup>e</sup>Department of Chemistry, Faculty of Science, Chulalongkorn University, Bangkok 10330, Thailand

<sup>f</sup>Siriraj Center of Research Excellence in Metabolomics and Systems Biology (SiCORE-MSB), Faculty of Medicine Siriraj Hospital, Mahidol University, Bangkok 10700, Thailand

<sup>g</sup>Siriraj Metabolomics and Phenomics Center, Faculty of Medicine Siriraj Hospital, Mahidol University, Bangkok 10700, Thailand

<sup>h</sup>Thailand Metabolomics Association, Bangkok 10700, Thailand

<sup>i</sup>Department of Biochemistry, Faculty of Medicine Siriraj Hospital, Mahidol University, Bangkok, Thailand

<sup>j</sup>Center of Excellence on Environmental Health and Toxicology (EHT), OPS, Ministry of Higher Education, Science, Research and Innovation, Bangkok 10400, Thailand

Furthermore, new SARS-CoV-2 variants continue to emerge even when the global vaccination coverage has increased,<sup>8,9</sup> resulting in lifelong health consequences if not adequately managed.<sup>10</sup>

Primary bile acids, including cholic acid and chenodeoxycholic acid, are synthesized in the liver directly from cholesterol through a multi-step enzymatic process and subsequently conjugated with glycine or taurine.<sup>11</sup> These conjugated bile acids are secreted into bile and released into the duodenum, where they aid in lipid digestion.<sup>12</sup> Approximately 15% escape *via* reabsorption in the terminal ileum and enter the colon, where gut microbiota deconjugate and convert them into secondary bile acids such as deoxycholic acid and lithocholic acid *via* 7 $\alpha$ -dehydroxylase.<sup>11,12</sup> A smaller fraction is further transformed into tertiary bile acids, such as ursodeoxycholic acid, through the activity of 7 $\beta$ -hydroxysteroid dehydrogenase.<sup>11</sup> Bile acids and bile salts are essential for the emulsification, digestion, and absorption of dietary lipids and fat-soluble vitamins.<sup>11</sup> Beyond their role in digestion, they also function in lipid and glucose metabolism, immune regulation, and antimicrobial defense.<sup>13–15</sup> Interestingly, lithocholic acid has been found to exhibit the anti-ageing effects of calorie restriction,<sup>16</sup> and it can bind to the TUB-like protein 3 (TULP3) to activate AMPK and sirtuins, and thus slowing down ageing.<sup>17</sup> In addition to these properties, bile acids and their conjugated forms have demonstrated inhibitory activity against a range of viruses, including rotavirus,<sup>18</sup> cytomegalovirus,<sup>19</sup> influenza A,<sup>20</sup> hepatitis B and D,<sup>21</sup> and porcine deltacoronavirus.<sup>22</sup> In the context of the SARS-CoV-2 virus, bile acids may interfere with the spike protein-ACE2 receptor interactions<sup>23</sup> and mediate downregulation of ACE2, and thus reduce susceptibility to SARS-CoV-2 infection.<sup>24</sup> Moreover, a recent review suggests that bile acids are effective in binding spike protein with the Angiotensin Converting Enzyme II (ACE2), thus preventing SARS-CoV-2 virus infection and replication.<sup>25</sup> Bile acids can also activate receptors, GPBAR1 and FXR, which may inactivate SARS-CoV-2 infection.<sup>25</sup> These preventive potentials of bile acids, as well as their receptors in the prevention (and treatment) of COVID-19, encourage us to investigate their antiviral and virucidal activities against SARS-CoV-2. These findings encourage us to explore the antiviral activity of bile acids and their salts against SARS-CoV-2.

Bald's Leechbook, a thousand-year-old Anglo-Saxon medical text written in Old English, documents a recipe containing bile from bullocks' gall, together with garlic, leeks, and wine, used for the treatment of infected eyelash follicles.<sup>26</sup> Bald's Leechbook has been found to have antibacterial and antibiofilm activities against methicillin-resistant *Staphylococcus aureus*.<sup>27</sup> Bile acid-based antimicrobials exert bactericidal effects against both Gram-positive and Gram-negative bacteria through multiple pathways, including binding to specific membrane targets, dissipation of membrane potential, pore formation in the cytoplasmic membrane, and induction of reactive oxygen species.<sup>28</sup> Many antimicrobial bile acid derivatives have been previously reported including deoxycholic acid-amino alcohol conjugates,<sup>29</sup> lithocholic acid derivatives,<sup>30</sup> di-substituted cholic acid-based peptides bearing cationic amino acids,<sup>31</sup> and cholic acid-derived amphiphiles.<sup>32,33</sup> These findings collectively

support the potential of bile acid derivatives as effective antimicrobial agents, encouraging us to investigate antimicrobial properties of bile acid derivatives in the form of salts.

Poor aqueous solubility remains a significant limitation for many bioactive compounds, particularly in pharmaceutical applications.<sup>34</sup> Salt formation is among the most common and effective strategies used to enhance aqueous solubility, with a large number of active pharmaceutical ingredients (APIs) currently marketed in salt form.<sup>34,35</sup> Bile acids possess inherently low aqueous solubility, whereas their corresponding bile salts demonstrate significantly enhanced solubility.<sup>36,37</sup> In recent years, organic counterions have gained popularity in modern pharmaceutical formulations due to their improved stability in aqueous environments.<sup>38</sup> A group of uniform materials based on organic salts (GUMBOS) are organic salts with tunable properties, such as fluoroquinolone-based organic salts GUMBOS, which displayed good antibacterial profiles with less cytotoxic activity,<sup>39</sup> targeting the bacterial DNA gyrase.<sup>40</sup> Recently, we reported that salts of alkaloids from the seed embryos of the lotus *Nelumbo nucifera* exhibit improved virucidal and antiviral activities against SARS-CoV-2.<sup>41</sup> Motivated by the unique properties of organic salts mentioned above, we investigated the antibacterial and antiviral activities of the bile acid salts. In the present work, the cations for bile acid salts were L-carnitine, creatinine, and choline, which are both endogenously synthesized in human body and are obtained through dietary intake.<sup>42</sup> L-carnitine plays a key role in fatty acid  $\beta$ -oxidation and carbohydrate metabolism, and it improves glucose disposal and mitigates fat accumulation in the body.<sup>43</sup> Creatinine is a metabolic end product derived from the spontaneous degradation of creatine and creatine phosphate in muscle tissue.<sup>44</sup> Creatinine can also be found in cooked meat and is widely used as a clinical biomarker for kidney function.<sup>44</sup> Choline, an essential nutrient, is found in a broad range of foods.<sup>45</sup> It is required for neurotransmitter synthesis, cell membrane signaling, lipid transport, and methyl group metabolism.<sup>46</sup> These three compounds are naturally present in the human body and abundant in common dietary sources. Their physiological relevance, safety, and widespread availability make them attractive, biocompatible, and accessible organic counterions for the development of bioactive bile acid salts.

The present work reports the synthesis of a series of bile acid salts by pairing four bile acids—lithocholic acid, deoxycholic acid, ursodeoxycholic acid, and chenodeoxycholic acid—with three naturally occurring organic cations: L-carnitine, creatinine, and choline. The synthesized bile acid salts were evaluated for their antiviral and virucidal activities against SARS-CoV-2 and for their antimicrobial properties.

## 2 Materials and methods

### 2.1 Chemicals

Lithocholic acid (LCA,  $\geq 98\%$ , TCI: L0089), deoxycholic acid (DCA,  $\geq 98\%$ , TCI: C0315), ursodeoxycholic acid (UDCA,  $\geq 98\%$ , TCI: U0030), chenodeoxycholic acid (CDCA,  $\geq 97\%$ , TCI: C0750), L-carnitine ( $\geq 98\%$ , TCI: C0049), and creatinine ( $\geq 99\%$ , TCI:



C0398) were purchased from Tokyo Chemical Industry Co., Ltd. Choline bicarbonate ( $\geq 99\%$ , Sigma-Aldrich: C7519) was obtained from Sigma-Aldrich. All chemicals were used as received.

## 2.2 Analysis of nuclear magnetic resonance (NMR) and differential scanning calorimetry (DSC)

NMR spectra were recorded on a Bruker AVANCE 400 MHz spectrometer (operating at 400 MHz for  $^1\text{H}$  NMR and 100 MHz for  $^{13}\text{C}$  NMR). HRESI-MS data were obtained using a Thermo Scientific (Q exactive focus) spectrometer. Approximately 4.3 mg of each sample was sealed in an aluminum pan (H aluminum seal). DSC experiments were performed using a Shimadzu DSC 60A Plus calorimeter. A sealed, empty pan served as the reference. Measurements were conducted under a nitrogen atmosphere at a flow rate of 50 mL min $^{-1}$ . The temperature program began with an isothermal hold at 45 °C for 1 min, followed by a linear heating ramp of 10 °C min $^{-1}$  to 280 °C. Each measurement was repeated at least twice.

## 2.3 Synthesis of bile acid salts

Salts of bile acids were prepared by reacting bile acids (lithocholic acid, deoxycholic acid, ursodeoxycholic acid, and chenodeoxycholic acid) with organic counterions, including L-carnitine, creatinine, and choline. Equimolar amounts of each bile acid (0.13 mmol; lithocholic acid, 48.95 mg; deoxycholic acid, 51.03 mg; ursodeoxycholic acid, 51.03 mg; chenodeoxycholic acid, 51.03 mg) were dissolved in 3 mL of methanol along with the corresponding organic counterion in a 1:1 molar ratio. Specifically, L-carnitine (0.13 mmol, 21 mg), creatinine (0.13 mmol, 15 mg), and choline bicarbonate (0.13 mmol, 23  $\mu\text{L}$  of 80% w/w aqueous solution, density 1.17 g mL $^{-1}$ ) were used for the salt formation of bile acids. The mixtures were stirred at room temperature overnight to promote salt formation. After completion, the reaction mixtures were evaporated to dryness using a rotary evaporator under reduced pressure and were subjected to vacuum drying overnight to ensure complete solvent removal.

## 2.4 Cell line and virus

Human epithelial lung carcinoma cells stably expressing human angiotensin I-converting enzyme 2 (A549-hACE2) and the SARS-CoV-2 Delta variant (B.1.617.2) were kindly provided by Dr Anan Jongkaewwattana (National Center for Genetic Engineering and Biotechnology, BIOTEC, Thailand).<sup>47</sup> A549-hACE2 cells were maintained in Dulbecco's Modified Eagle's Medium (DMEM)/high glucose (Cytiva, Marlborough, MA, USA), supplemented with 10% fetal bovine serum (FBS; Sigma, St. Louis, MO, USA) and antibiotics. Viral stocks were prepared by propagating SARS-CoV-2 in A549-hACE2 cells. Supernatants containing progeny virions were collected, clarified, and stored at  $-80\text{ }^\circ\text{C}$  until use. All experiments involving SARS-CoV-2 were conducted in a biosafety level 3 (BSL-3) facility at BIOTEC, Thailand.

## 2.5 Cytotoxicity assay

A549-hACE2 cells, the host cell line for SARS-CoV-2 infection used in both virucidal and antiviral assays, were assessed for cytotoxicity of test compounds as previously described.<sup>41,48</sup> Briefly, cells were seeded into 96-well plates overnight at a density of  $4 \times 10^4$  cells per well. For cytotoxicity testing in the context of the virucidal assay, cells were pre-treated with the indicated concentrations of the compounds at 37 °C for 1 h, followed by culturing in fresh medium without compounds for 72 h. For the antiviral assay, cytotoxicity was evaluated by treating cells with the indicated compound concentrations at 37 °C for 72 h. Following treatment, the viability of the cells was measured by determining cellular ATP levels using the CellTiter-Glo Assay (Promega, Madison, WI, USA). Luminescence was quantified using an EnSight Multimode Plate Reader (PerkinElmer, Waltham, MA, USA). Dimethyl sulfoxide (DMSO)-treated cells served as the control, representing 100% cell viability.

## 2.6 Virucidal and antiviral assays

The inhibitory effects of the test compounds on SARS-CoV-2 were assessed via virucidal and antiviral assays, as previously described.<sup>41,48</sup> Briefly, A549-hACE2 cells were seeded in 96-well plates at  $4 \times 10^4$  cells per well and incubated overnight. In the virucidal assay, viral particles were pre-treated with the test compounds at the indicated concentrations for 1 h at 37 °C. The treated virus was then added to the cells and incubated for 1 h at 37 °C to allow viral adsorption. Afterward, the cells were cultured in fresh medium without compounds for 72 h. In the antiviral assay, cells were first infected with SARS-CoV-2 for 1 h at 37 °C. Following infection, cells were cultured in medium containing the indicated concentrations of test compounds for 72 h. To assess viral infectivity, cytopathic effects were quantified using the Viral ToxGlo Assay (Promega), and luminescence signals were measured with the EnSight Multimode Plate Reader. In the virucidal assay, DMSO-treated virus served as the 100% viral infectivity control. In the antiviral assay, infected cells treated with DMSO were used as the 100% viral infectivity control. The anti-SARS-CoV-2 spike antibody (anti-S), monoRab SARS-CoV-2 neutralizing antibody BS-R2B2 (GenScript, Piscataway, NJ, USA), which targets the viral particle to block infection, and ethanol, which directly disrupts the viral envelope, were used as positive controls in the virucidal assay.

## 2.7 Antibacterial and antifungal testing

The antibacterial activity of twelve synthesized bile salt derivatives and bile acids was evaluated using the disc diffusion method. Microorganisms used for antimicrobial activity testing were purchased from the Thailand Institute of Scientific and Technological Research (TISTR), Thailand, except *Shigella flexneri* from the ATCC (American Type Culture Collection, ATCC). The microorganisms used in this work were *Bacillus cereus* TISTR035, *Staphylococcus aureus* TISTR746, *Staphylococcus epidermidis* TISTR2172, *Enterococcus faecalis* TISTR927, *Escherichia coli* TISTR117, *Pseudomonas aeruginosa* TISTR357, *Salmonella*



*enterica* serovar Typhimurium TISTR1470, *S. flexneri* ATCC 9199, and *Candida albicans* TISTR5554. Test compounds were dissolved in DMSO at the appropriate concentration. Sterile paper discs (6 mm in diameter) were impregnated with 1 mg of each compound. For each plate, four treatment zones were prepared: a negative control (DMSO), a positive control (5 µg per disc of ciprofloxacin for bacterial strains or 10 µg per disc of amphotericin B for *C. albicans*), the free bile acid, and the bile salt derivatives. The discs were then placed on nutrient agar plates previously inoculated with a standardized bacterial suspension (adjusted to 0.5 McFarland standard). Plates were incubated at 37 °C for 18–24 h, after which the zones of inhibition were measured in millimeters (mm). Each assay was conducted in triplicate to ensure reproducibility.

## 2.8 Statistical analysis

All experiments were performed with at least three independent biological replicates. Data are presented as mean  $\pm$  standard deviation (SD), as indicated in figure legends. Half-maximal effective concentration ( $EC_{50}$ ) and half-maximal cytotoxic concentration ( $CC_{50}$ ) values were determined by fitting dose-response curves using nonlinear regression (log[inhibitor] vs. normalized response-variable slope) in GraphPad Prism software (version 9.0; GraphPad Software, San Diego, CA, USA). The selectivity index (SI) for each compound was calculated as the ratio of  $CC_{50}$  to  $EC_{50}$  ( $SI = CC_{50}/EC_{50}$ ).

## 3 Results and discussion

### 3.1 Preparation of bile acid salts

Inspired by previous works on the synthesis of bile acid salts, such as choline cholate and choline deoxycholate-based biosurfactants,<sup>49</sup> and fluoroquinolone-based organic salts (GUMBOS) as antimicrobial agents,<sup>39,40,50</sup> we prepared bile acid salts of lithocholic acid (LCA, 1), deoxycholic acid (DCA, 5), ursodeoxycholic acid (UDCA, 9), and chenodeoxycholic acid (CDCA, 13) with three organic cations: L-carnitine, creatinine, and choline, denoted as [X], [Y], and [Z], respectively (Fig. 1). The structures of creatinine and creatininium cations were adopted from a previous study.<sup>51</sup> We hypothesized that these bile acid salts might exhibit antiviral and antimicrobial activities or even possess enhanced activity compared to their corresponding bile acids. The salts of bile acids were prepared following the previous method for choline cholate and choline deoxycholate using equimolar amounts of each bile acid and the corresponding organic counterion (1 : 1 molar ratio).<sup>49</sup> The cationic ions used in this work include L-carnitine ion [X], creatininium ion [Y], and cholinium ion [Z] (Fig. 1). The bile acid LCA (1) reacted with the cationic ions [X], [Y], and [Z], yielding the corresponding salts [LCA][X] (2), [LCA][Y] (3), and [LCA][Z] (4), while DCA (5) provided the salts [DCA][X] (6), [DCA][Y] (7), and [DCA][Z] (8), respectively (Fig. 1). Similarly, the bile acid UDCA (9) yielded the salts [UDCA][X] (10), [UDCA][Y] (11), and [UDCA][Z] (12), and the acid CDCA (13) formed the salts [CDCA][X] (14), [CDCA][Y] (15), and [CDCA][Z] (16) (Fig. 1). The  $^1H$  NMR spectra of the individual bile acid salts, e.g., compounds 2–4, 6–8, 10–

12, and 14–16, showed signals consistent with a 1 : 1 ratio of the individual bile acid and its corresponding cation. Detailed  $^1H$  and  $^{13}C$  NMR data of bile acid salts, as well as their NMR spectra, are provided in the SI. DSC thermogram of salts 2–4 showed melting points in the range of 174.06–195.80 °C, while salts 6 and 7 had melting points of 185.91 and 250.81 °C, respectively. The DSC data for the cholinium salt [DCA][Z] (8) were previously reported, showing a melting point of 238.77 °C.<sup>49</sup> Salts 14–16 exhibited melting point in the range of 187.26–252.34 °C. DSC thermograms and data for all salts, except [DCA][Z] (8), are included in the SI. ESI-MS analysis of the synthesized bile acid salts is summarized in Table S1 of the SI.

### 3.2 Antiviral and virucidal activities against SARS-CoV-2

Our previous work demonstrated that organic salts had an influence on biological activities because salts of alkaloids from *N. nucifera* exhibited improved virucidal activity against SARS-CoV-2 with less cytotoxicity.<sup>41</sup> In the present work, bile acids and their salts (compounds 1–16, Fig. 1) were evaluated for their antiviral and virucidal activities against SARS-CoV-2. Virucidal activity was evaluated by pre-treating SARS-CoV-2 particles with test compounds, while antiviral activity was assessed by infecting the host cells with the virus, followed by treatment with each sample for 72 h.<sup>41,48</sup> It was found that bile acids LCA (1), DCA (5), UDCA (9), and CDCA (13), and their salts 2–4, 6–8, 10–12, and 14–16 did not exhibit antiviral activity toward SARS-CoV-2. However, LCA (1) was found to have virucidal activity against SARS-CoV-2 (Fig. 2). Bright-field microscopy showed inhibition of cytopathic effect by LCA (1) and by the positive controls for virucidal activity: ethanol and anti-SARS-CoV-2 spike antibody (Fig. 2A). Viral infectivity and cytotoxicity of LCA (1) are displayed in Fig. 2B and C. While LCA (1) did not show cytotoxicity at the tested concentrations (Fig. 2C), it showed

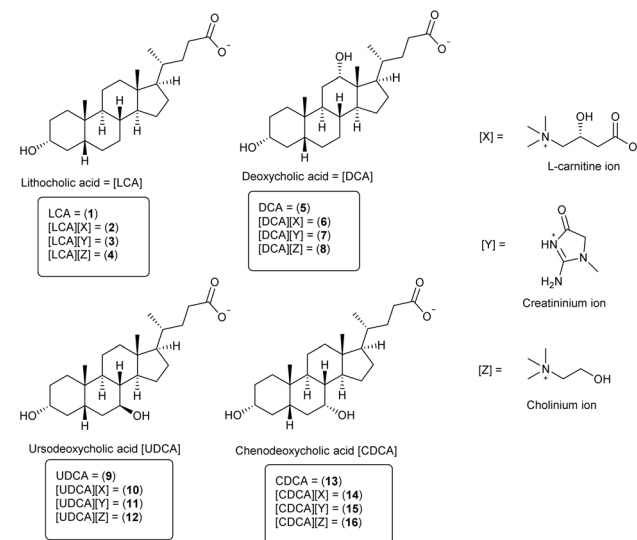
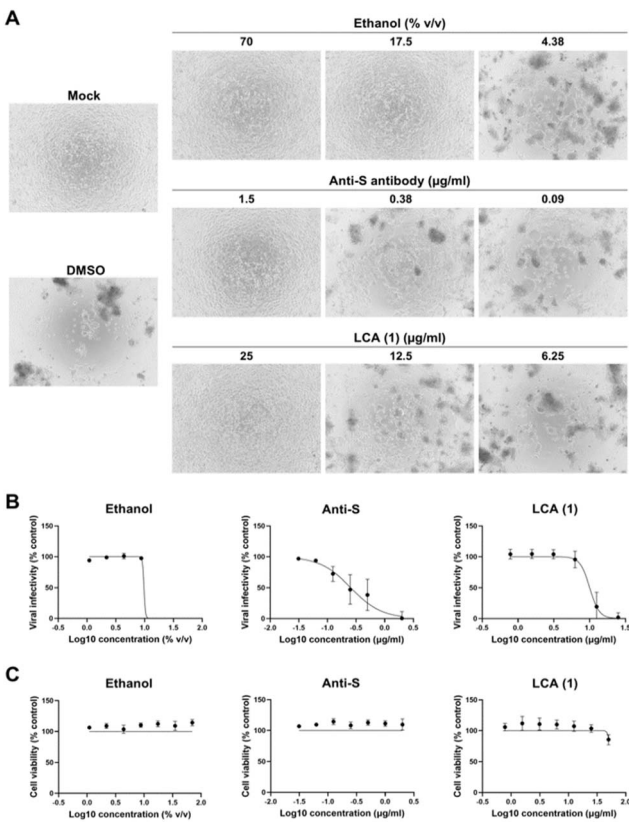


Fig. 1 Salts of the bile acids, namely, lithocholic acid (LCA), deoxycholic acid (DCA), ursodeoxycholic acid (UDCA), and chenodeoxycholic acid (CDCA), with the organic cations of L-carnitine, creatinine, and choline, represented as [X], [Y], and [Z], respectively.





**Fig. 2** Virucidal effect and cytotoxicity of LCA (1). (A and B) SARS-CoV-2 particles were pre-treated with LCA (1) for 1 h and subsequently used to infect A549-hACE2 cells. At 72 h post infection, cytopathic effects were observed by bright-field microscopy (A), and cell viability was assessed using the Viral ToxGlo assay (B). Mock refers to uninfected cells, while cells infected with the untreated virus served as the 100% viral infectivity control. (C) Cytotoxicity of LCA (1) was evaluated by treating A549-hACE2 cells with the compound for 1 h, followed by culture in medium without compound for 72 h. Cell viability was determined using the CellTiter-Glo assay. Untreated cells were used as the 100% cell viability control. Data represent mean  $\pm$  SD from at least 3 independent experiments (each performed in duplicate) and were fitted to dose-response curves using GraphPad Prism software.

virucidal activity against SARS-CoV-2 with an  $EC_{50}$  of  $9.69 \mu\text{g mL}^{-1}$  and an  $SI > 5.16$  (Table 1). Note that the positive control anti-S, which is considered the best neutralizing agent against SARS-CoV-2 virus, exhibited virucidal activity with an  $EC_{50}$  value of  $0.30 \mu\text{g mL}^{-1}$  and an  $SI$  of 6.63 (Table 1), making it 32.3 times more potent than LCA (1). Another positive control,

**Table 1** Virucidal activity of LCA (1) and its salts 2–4 against SARS-CoV-2

Sample	$EC_{50}$	$CC_{50}$	SI
LCA (1)	$9.69 \pm 2.26 \mu\text{g mL}^{-1}$	$>50 \mu\text{g mL}^{-1}$	$>5.16$
[LCA][X] (2)	$21.92 \pm 5.24 \mu\text{g mL}^{-1}$	$>50 \mu\text{g mL}^{-1}$	$>2.28$
[LCA][Y] (3)	$12.73 \pm 2.72 \mu\text{g mL}^{-1}$	$>50 \mu\text{g mL}^{-1}$	$>3.93$
[LCA][Z] (4)	$31.73 \pm 4.72 \mu\text{g mL}^{-1}$	$>50 \mu\text{g mL}^{-1}$	$>1.58$
Anti-S (positive control)	$0.30 \pm 0.14 \mu\text{g mL}^{-1}$	$>2 \mu\text{g mL}^{-1}$	$>6.63$
Ethanol (positive control)	$9.45\% \pm 2.61\% \text{ v/v}$	$>70\% \text{ v/v}$	$>7.41$

ethanol, a common effective disinfectant against viruses, showed an  $EC_{50}$  value of  $9.45\% \text{ v/v}$  with an  $SI > 7.41$  (Table 1).

According to our previous work showing improved virucidal activity of alkaloid salts against SARS-CoV-2,<sup>41</sup> we then evaluated the virucidal activity of LCA (1) salts. Fig. 3 shows virucidal activity and cytotoxicity of LCA (1) salts including [LCA][X] (2), [LCA][Y] (3), and [LCA][Z] (4). Again, the salts [LCA][X] (2), [LCA][Y] (3), and [LCA][Z] (4) did not exhibit cytotoxicity at the tested concentrations (Fig. 3), and they displayed virucidal activity against SARS-CoV-2 with  $EC_{50}$  values of  $21.92$ ,  $12.73$ , and  $31.73 \mu\text{g mL}^{-1}$ , respectively (Table 1). Note that the virucidal activities of salts 2–4 were  $2.26$ ,  $1.31$ , and  $3.27$  times lower, respectively, than those of the free acid LCA (1), indicating that salts of this bile acid did not improve virucidal activity. Moreover, the  $SI$  values of salts 2–4 ( $1.58$ – $3.93$ ) were lower than that of the free acid LCA (1) ( $SI = 5.16$ ) (Table 1). Overall, the salts of LCA (1) did not show improved virucidal activity or  $SI$  against SARS-CoV-2.

Recently, the bile acid LCA (1) in combination with its oleate derivative was reported to exhibit both *in vitro* and *in vivo* antiviral activities against human herpes simplex virus 1 (HSV-1).<sup>52</sup> LCA (1), produced by gut microbiota, was found to have an anti-infective role in protecting piglets against porcine epidemic diarrhea virus (PEDV) infection.<sup>53</sup> A separate study revealed that LCA (1) potentially inhibited porcine deltacoronavirus (PDCoV) infection in piglets by targeting the cellular receptor aminopeptidase N.<sup>54</sup> A propargylaminoalkyl derivative of LCA (1) exhibited antiviral activity against the influenza H1N1 virus.<sup>55</sup> *In vitro* models showed that the bile acids LCA (1) and CDCA (13) were found to be antiviral agents against PDCoV in a porcine kidney cell line.<sup>56</sup> To our knowledge, this is the first report of the antiviral activity of LCA (1) against SARS-CoV-2.

The infection inhibition of CDCA (13) against vesiculovirus (VSV) was enhanced by inhibiting the farnesoid X receptor

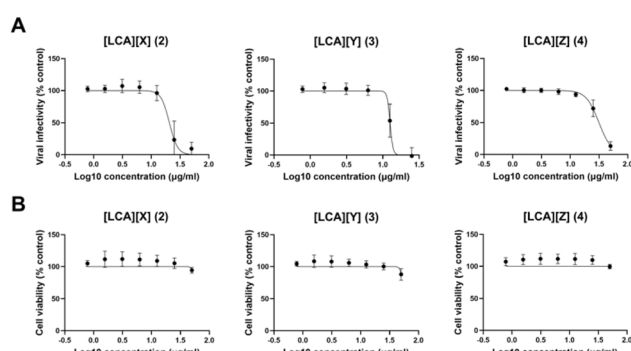


**Fig. 3** Virucidal activity of [LCA][X] (2), [LCA][Y] (3), and [LCA][Z] (4). (A) Virucidal activity of test compounds was evaluated by pre-treating SARS-CoV-2 particles with each compound for 1 h prior to the infection of A549-hACE2 cells. At 72 h post infection, viral cytopathic effects were quantified using the Viral ToxGlo assay. Cells infected with untreated virus served as the 100% viral infectivity control. (B) Cytotoxicity of the test compounds was assessed by treating A549-hACE2 cells for 1 h, followed by incubation in medium without compound for 72 h. Cell viability was measured using the CellTiter-Glo assay. Untreated cells were used as the 100% cell viability control. Dose-response data are presented as mean  $\pm$  SD from at least 3 independent experiments, each performed in duplicate.



(FXR).<sup>57</sup> DCA (5) was previously reported to inhibit African swine fever (ASF) virus replication by suppressing MAPK signaling pathway,<sup>58</sup> and DCA (5) has been found in traditional Chinese medicine recommended for the treatment of COVID-19.<sup>59</sup> DCA (5) restores plasmacytoid dendritic cell (pDC) functions and type I interferon (IFN) responses to restrict Chikungunya virus dissemination.<sup>60</sup> Previously, UDCA (9) has been reported as an FXR antagonist that can downregulate ACE2; it could prevent SARS-CoV-2 Delta variant *in vivo*.<sup>24</sup> The combination of UDCA (9) and the gut bacterium *Bifidobacterium* could reduce the levels of virological markers in patients with chronic hepatitis B, thus improving liver function.<sup>61</sup> For patients with chronic liver diseases who are diagnosed with SARS-CoV-2 infection, UDCA (9) may improve clinical outcomes.<sup>62</sup> In a separate study, UDCA (9) has been shown to shorten recovery time in patients infected with Omicron strain of SARS-CoV-2 infection.<sup>63</sup> Normally, UDCA (9) is used as a drug to treat chronic cholestatic liver diseases, *e.g.*, primary biliary cholangitis. A cohort study using the OpenSAFELY platform revealed that UDCA (9) could reduce the risk of severe COVID-19 outcomes, thus preventing serious illness of COVID-19 patients.<sup>64</sup> UDCA (9) and CDCA (13) have interactions with the receptors GPBAR1 and FXR, effectively modulating the expression of ACE2, and therefore, they have potential for anti-COVID-19 therapies.<sup>25</sup> CDCA (13) can inhibit influenza A virus replication *in vitro*, at least in part, by blocking the nuclear export of viral ribonucleoprotein complexes.<sup>20</sup> Network pharmacology analyses suggest that CDCA (13) may be useful for the treatment of acute lung injury, and an animal model proved that it can ameliorate pathological injury to lung tissues in mice.<sup>65</sup> This suggests that CDCA (13) may help patients with serious respiratory illness caused by SARS-CoV-2 infection. However, the present work showed that DCA (5),

UDCA (9), and CDCA (13) did not exhibit antiviral or virucidal activity against SARS-CoV-2.

### 3.3 Antibacterial and antifungal properties

Bile salts are known to have potent antimicrobial activity, and previous work have shown that they exhibited antibacterial activity against *Staphylococcus aureus*, an opportunistic bacterial pathogen responsible for many infections.<sup>66</sup> In the present work, it was found that bile acids and their salts showed antibacterial activity against Gram-positive bacteria, including *B. cereus*, *S. aureus*, *S. epidermidis*, and *E. faecalis*, and that they selectively displayed activity against the Gram-negative bacterium, *E. coli* (Table 2). The bile acid LCA (1) was found inactive against *B. cereus*; however, its cholinium salt, [LCA][Z] (4), showed antibacterial activity toward *B. cereus* with an inhibition zone of 7.8 mm (Table 2), suggesting that the salt form can improve antibacterial activity. A bile acid DCA (5) showed activity against *B. cereus*, *S. aureus*, *S. epidermidis*, *E. faecalis*, and *E. coli*, with inhibition zones of 10.6–14.4 mm, while its cholinium salt, [DCA][Z] (8), exhibited improved antibacterial activity, with inhibition zones of 13.0–19.1 mm (Table 2). The significant activity improvements for the [DCA][Z] (8) salt were observed against *S. epidermidis* and *E. faecalis*, showing respective inhibition zones of 19.1 and 15.0 mm, respectively, while the bile acid DCA (5) displayed less activity against these bacteria, with inhibition zones of 13.5 and 10.6 mm. Therefore, the [DCA][Z] (8) salt exhibited a 41.4–41.5% improvement in antibacterial activity compared to its bile acid DCA (5). The bile acid UDCA (9) exhibited activity against *B. cereus*, *S. aureus*, *S. epidermidis*, and *E. coli*, but was inactive against the bacterium *E. faecalis*. While the bile acid UDCA (9) exhibited antibacterial

Table 2 Antimicrobial activity of bile acids and their salts expressed as inhibition zone diameters (mm) with standard deviations (SD)

	Inhibition zone $\pm$ SD (mm)								Fungus	
	Gram-positive bacteria				Gram-negative bacteria					
	<i>B. cereus</i>	<i>S. aureus</i>	<i>S. epidermidis</i>	<i>E. faecalis</i>	<i>E. coli</i>	<i>P. aeruginosa</i>	<i>S. typhi</i>	<i>S. flexneri</i>		
Positive control <sup>a</sup>	33.2 $\pm$ 1.6	31.0 $\pm$ 1.5	36.4 $\pm$ 0.4	24.1 $\pm$ 1.0	38.5 $\pm$ 2.1	31.2 $\pm$ 1.1	39.3 $\pm$ 2.6	42.1 $\pm$ 0.7	21.8 $\pm$ 1.3	
LCA (1)	Inactive	Inactive	Inactive	Inactive	Inactive	Inactive	Inactive	Inactive	Inactive	
[LCA][X] (2)	Inactive	Inactive	Inactive	Inactive	Inactive	Inactive	Inactive	Inactive	Inactive	
[LCA][Y] (3)	Inactive	Inactive	Inactive	Inactive	Inactive	Inactive	Inactive	Inactive	Inactive	
[LCA][Z] (4)	7.8 $\pm$ 1.2	Inactive	Inactive	Inactive	Inactive	Inactive	Inactive	Inactive	Inactive	
DCA (5)	14.4 $\pm$ 1.5	11.7 $\pm$ 1.6	13.5 $\pm$ 0.7	10.6 $\pm$ 0.4	10.9 $\pm$ 1.6	Inactive	Inactive	Inactive	Inactive	
[DCA][X] (6)	13.6 $\pm$ 1.4	10.8 $\pm$ 2.5	12.3 $\pm$ 0.3	9.8 $\pm$ 1.2	9.5 $\pm$ 0.4	Inactive	Inactive	Inactive	Inactive	
[DCA][Y] (7)	14.7 $\pm$ 0.5	11.5 $\pm$ 1.8	13.3 $\pm$ 0.2	11.2 $\pm$ 1.1	10.9 $\pm$ 1.0	Inactive	Inactive	Inactive	Inactive	
[DCA][Z] (8)	18.1 $\pm$ 1.7	15.4 $\pm$ 2.0	19.1 $\pm$ 0.2	15.0 $\pm$ 1.3	13.0 $\pm$ 1.9	Inactive	Inactive	Inactive	Inactive	
UDCA (9)	8.7 $\pm$ 0.3	7.8 $\pm$ 0.8	9.6 $\pm$ 0.4	Inactive	7.4 $\pm$ 0.4	Inactive	Inactive	Inactive	Inactive	
[UDCA][X] (10)	8.7 $\pm$ 0.5	7.8 $\pm$ 0.6	9.2 $\pm$ 0.7	Inactive	7.9 $\pm$ 0.1	Inactive	Inactive	Inactive	Inactive	
[UDCA][Y] (11)	8.1 $\pm$ 1.0	7.2 $\pm$ 0.2	8.5 $\pm$ 0.6	Inactive	7.1 $\pm$ 0.1	Inactive	Inactive	Inactive	Inactive	
[UDCA][Z] (12)	12.5 $\pm$ 0.5	10.3 $\pm$ 1.7	13.0 $\pm$ 0.5	Inactive	10.1 $\pm$ 1.1	Inactive	Inactive	Inactive	Inactive	
CDCA (13)	13.5 $\pm$ 0.4	9.4 $\pm$ 0.8	11.8 $\pm$ 0.4	8.4 $\pm$ 1.1	7.6 $\pm$ 0.6	Inactive	Inactive	Inactive	Inactive	
[CDCA][X] (14)	11.5 $\pm$ 0.7	8.9 $\pm$ 0.2	11.4 $\pm$ 0.5	7.7 $\pm$ 0.6	7.7 $\pm$ 1.1	Inactive	Inactive	Inactive	Inactive	
[CDCA][Y] (15)	12.4 $\pm$ 0.7	9.5 $\pm$ 0.5	12.0 $\pm$ 0.6	8.2 $\pm$ 0.9	7.3 $\pm$ 0.2	Inactive	Inactive	Inactive	Inactive	
[CDCA][Z] (16)	16.4 $\pm$ 0.7	13.8 $\pm$ 1.3	17.1 $\pm$ 0.5	12.2 $\pm$ 2.6	10.4 $\pm$ 1.2	Inactive	Inactive	Inactive	Inactive	

<sup>a</sup> Positive control: ciprofloxacin, 5  $\mu$ g per disc for bacterial strains or amphotericin B, 10  $\mu$ g per disc for antifungal activity against *C. albicans*.



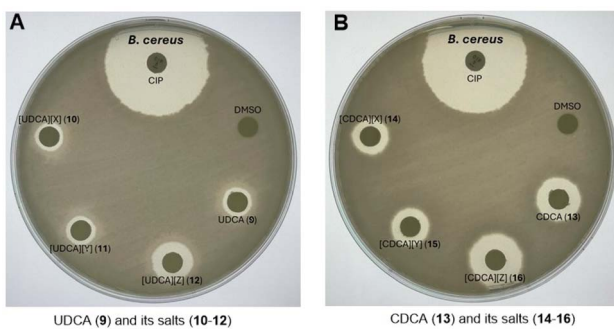


Fig. 4 Examples of antibacterial activity testing against *B. cereus* using the disc diffusion method. (A) Enhanced activity of the cholinium salt [UDCA][Z] (12) compared with UDCA (9). (B) Enhanced activity of the cholinium salt [CDCA][Z] (16) compared with CDCA (13).

activity with inhibition zones of 7.4–9.6 mm against Gram-positive bacteria, except *E. faecalis*, its cholinium salt [UDCA][Z] (12) displayed improved activity, with inhibition zones of 10.1–13.0 mm (Table 2). CDCA (13) showed antibacterial activity against Gram-positive bacteria *B. cereus*, *S. aureus*, *S. epidermidis*, and *E. faecalis* and the Gram-negative bacterium *E. coli*, with inhibition zones of 13.5, 9.4, 11.8, 8.4, and 7.6 mm, respectively, while its cholinium salt [CDCA][Z] (16) clearly exhibited improved activity, with inhibition zones of 16.4, 13.8, 17.1, 12.2, and 10.4 mm (Table 2). Representative images of antibacterial activity testing against *B. cereus* for bile acids, UDCA (9) and CDCA (13), and their salts are shown in Fig. 4, which demonstrates the improved antibacterial properties of their cholinium salts, [UDCA][Z] (12) and [CDCA][Z] (16). Additional images for antibacterial activity testing against *B. cereus*,

*S. aureus*, *S. epidermidis*, *E. faecalis*, and *E. coli* for other compounds are provided in the SI (Fig. S25–S29).

Fig. 5 shows a heat map comparing the magnitude of antibacterial activity of the bile acids LCA (1), DCA (5), UDCA (9), and CDCA (13) with their corresponding salts. Within the same bacterial strain, the heat map clearly shows that the corresponding cholinium salts of individual bile acids, *e.g.*, [LCA][Z] (4), [DCA][Z] (8), [UDCA][Z] (12), and [CDCA][Z] (16), exhibit better antibacterial activity than bile acids, LCA (1), DCA (5), UDCA (9), and CDCA (13), respectively (Fig. 5). Previously, a group of uniform materials based on organic salts (GUMBOS) was found to have antimicrobial properties with the potential to be used against antimicrobial resistance.<sup>50</sup> Fluoroquinolone-based organic salts display antibacterial activity by targeting bacterial DNA gyrase.<sup>40</sup> The salt of the gatifloxacin drug with *p*-coumaric acid showed improved oral bioavailability and antibacterial activity,<sup>67</sup> while salts of the drug gatifloxacin with ferulic acid and vanillic acid exhibited increased antibacterial activity.<sup>68</sup> Recently, organic salts of the old drug, streptomycin, were found to display enhanced antimicrobial efficacy and biocompatibility. Dicarboxylate salts of the antibiotic drug levofloxacin demonstrated better potency, solubility, and stability compared to levofloxacin alone.<sup>69</sup> These previous works demonstrate that salt forms of certain compounds or drugs can enhance antibacterial activity. The present work supports that certain organic salts can improve antibacterial activity, for example, cholinium salts of the bile acids investigated in this work. Although organic salts of bile acids show improved antibacterial activity, their salt forms do not exhibit enhanced antiviral or virucidal activity against SARS-CoV-2.

Although this work demonstrated that the cholinium salts of bile acids exhibited enhanced antibacterial activity, there are

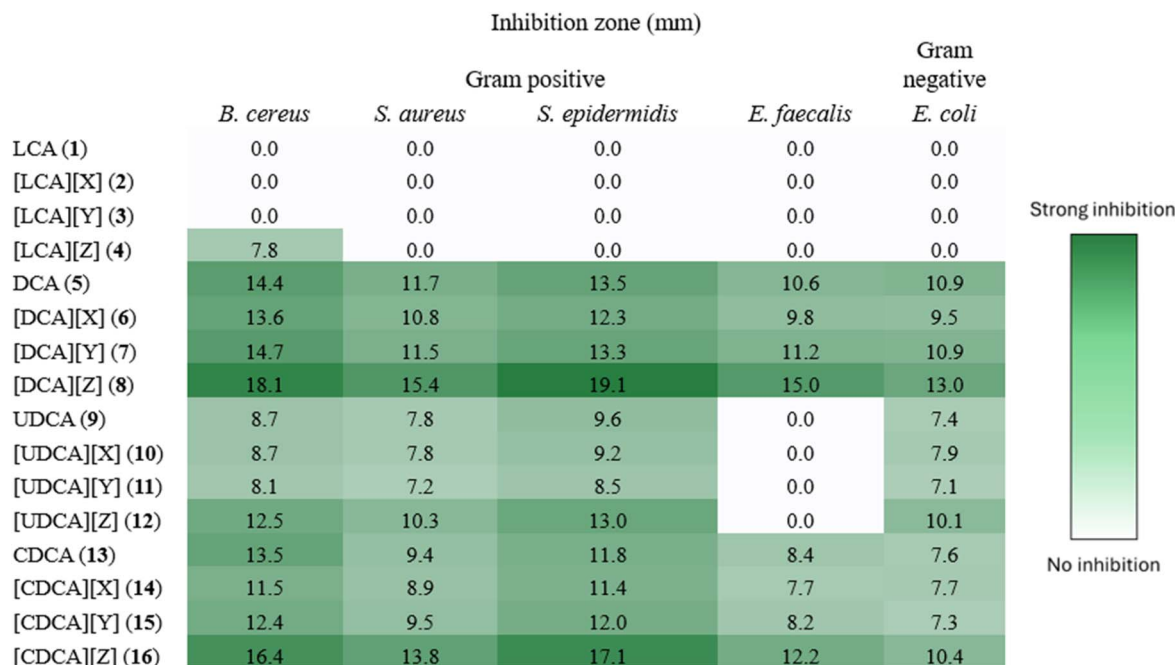


Fig. 5 Heat map representing the antibacterial activity of bile acids (1, 5, 9, and 13) and their salts (2–4, 6–8, 10–12, and 14–16).



limitations in the present work: (1) the formation of salts, particularly those with the L-carnitine ion [X] and creatininium ion [Y], could not be fully demonstrated; X-ray analysis of the salt structures should be used to confirm their structures; (2) the antibacterial mechanism of the cholinium salts was not investigated; (3) the virucidal mechanism of lithocholic acid (LCA, 1) against SARS-CoV-2 is not known. Further studies are needed to answer these questions.

It is interesting to note that only lithocholic acid (LCA, 1) was found to display virucidal activity against SARS-CoV-2, while deoxycholic acid (DCA, 5), ursodeoxycholic acid (UDCA, 9), and chenodeoxycholic acid (CDCA, 13) did not show activity. LCA (1) has a hydroxyl group at C-3, whereas DCA (5), UDCA (9), and CDCA (13) have two hydroxyl groups at C-3 and other positions (Fig. 1). Therefore, an additional hydroxyl moiety leads to the diminished antiviral activity of bile acids. In contrast, the heat map representing antibacterial activity (Fig. 5) indicates that bile acids DCA (5), UDCA (9), and CDCA (13) and their salts generally exhibit better antibacterial activity than LCA (1), suggesting that an additional hydroxyl functional group is essential for antibacterial activity.

Cholinium salts of bile acids are quaternary ammonium amphiphiles. The cationic charge of quaternary ammonium amphiphiles is important for antibacterial activity and biofilm eradication.<sup>70</sup> Previously, cholinium-based ionic liquids were found to show antibiofilm activity by disruption of the extracellular polymeric matrix through electrostatic interactions, thus causing bacterial cell death.<sup>71</sup> A Previous study on the antibacterial mechanism of action of choline-geranate ionic liquids revealed that choline could bind to the negatively charged bacterial cell membrane, thus inserting the geranate molecule into the lipid bilayer.<sup>72</sup> Therefore, we propose that the antibacterial mechanism of cholinium salts of bile acids may be through the electrostatic interactions of cholinium ion and bacterial cell membrane, probably disrupting the lipid bilayer of the cell membrane and leading to bacterial cell death.

## 4 Conclusions

Recently, there have been a number of previous works on bile acids with different aspects. The present work demonstrated the antiviral, virucidal, and antimicrobial activities of bile acids and their salts against the SARS-CoV-2 virus. Lithocholic acid, LCA (1), showed virucidal activity against SARS-CoV-2; however, its salts, [LCA][X] (2), [LCA][Y] (3), and [LCA][Z] (4), did not show enhanced virucidal activity. Although LCA (1) displayed virucidal activity, it did not show antibacterial activity. However, a cholinium salt of LCA (1), *i.e.*, [LCA][Z] (4), exhibited antibacterial activity, suggesting that cholinium salts can improve antibacterial activity. Bile acids, DCA (5), UDCA (9), and CDCA (13), showed antibacterial activity, while cholinium ion salts of these bile acids, *i.e.*, [DCA][Z] (8), [UDCA][Z] (12), and [CDCA][Z] (16), exhibited enhanced antibacterial activity. These results support that cholinium salts of bile acids can enhance antibacterial activity. This work adds to the importance of salts of organic compounds as a source of bioactive agents.

## Author contributions

C. V.: investigation, formal analysis, writing – original draft; N. C.: investigation, formal analysis, writing – original draft; N. L.: investigation, formal analysis; S. S.: formal analysis; T. P.: formal analysis; T. A.: formal analysis; S. K.: formal analysis; C. M.: supervision; S. R.: supervision; P. K.: conceptualization, funding acquisition, writing – original draft, writing – review & editing.

## Conflicts of interest

There are no conflicts to declare.

## Data availability

Data will be made available on request.

Supplementary information (SI): <sup>1</sup>H and <sup>13</sup>C NMR spectra and data of bile acid salts; ESI-MS analysis; DSC thermogram of salts; and pictures of disc diffusion assay. See DOI: <https://doi.org/10.1039/d5ra07917a>.

## Acknowledgements

P. Kittakoop would like to acknowledge the grant funded by the National Research Council of Thailand (NRCT), Contract number no.42A670689, the National Science, Research and Innovation Fund (NSRF), and Thailand Science Research and Innovation (TSRI). This work is supported in part by the grant from the Center of Excellence on Environmental Health and Toxicology (EHT), OPS, Ministry of Higher Education, Science, Research and Innovation. We acknowledge the financial support and facilities of the Chulabhorn Research Institute (CRI) and the Chulabhorn Graduate Institute (CGI), as well as the grant from the NRCT, NSRF and TSRI. C. Varongkriengkrai thanks the grant from the Chulabhorn Graduate Institute Scholarship CGS (2023)/10. We appreciate Dr Anan Jongkaew-wattana for providing SARS-CoV-2 for virucidal and antiviral assays.

## Notes and references

- 1 Coronavirus disease (COVID-19), [https://www.who.int/news-room/fact-sheets/detail/coronavirus-disease-\(covid-19\)](https://www.who.int/news-room/fact-sheets/detail/coronavirus-disease-(covid-19)), accessed May 16, 2025.
- 2 WHO COVID-19 dashboard, <https://data.who.int/dashboards/covid19/deaths?n=c>, accessed May 16, 2025.
- 3 Y. Miyah, M. Benjelloun, S. Lairini and A. Lahrichi, *Sci. World J.*, 2022, **2022**, 5578284.
- 4 S. S. Priya, C. Erdem and K. Sudhakar, *Int. J. Sustain. Eng.*, 2021, **14**, 1290–1305.
- 5 S. Naseer, S. Khalid, S. Parveen, K. Abbass, H. Song and M. V. Achim, *Front. Public Health*, 2023, **10**–2022, 1009393.
- 6 C. Zheng, W. Shao, X. Chen, B. Zhang, G. Wang and W. Zhang, *Int. J. Infect. Dis.*, 2022, **114**, 252–260.
- 7 A. I. Francis, S. Ghany, T. Gilkes and S. Umakanthan, *Postgrad. Med. J.*, 2021, **98**, 389–394.



8 A. M. Carabelli, T. P. Peacock, L. G. Thorne, W. T. Harvey, J. Hughes, T. I. de Silva, S. J. Peacock, W. S. Barclay, T. I. de Silva, G. J. Towers, D. L. Robertson and C.-G. U. Consortium, *Nat. Rev. Microbiol.*, 2023, **21**, 162–177.

9 S. S. A. Karim and Q. A. Karim, *Lancet*, 2021, **398**, 2126–2128.

10 H. E. Davis, L. McCorkell, J. M. Vogel and E. J. Topol, *Nat. Rev. Microbiol.*, 2023, **21**, 133–146.

11 A. Macierzanka, A. Torcello-Gómez, C. Jungnickel and J. Maldonado-Valderrama, *Adv. Colloid Interface Sci.*, 2019, **274**, 102045.

12 A. Di Ciaula, G. Garruti, R. Lunardi Baccetto, E. Molina-Molina, L. Bonfrate, D. Q. H. Wang and P. Portincasa, *Ann. Hepatol.*, 2017, **16**, S4–S14.

13 B. Staels and V. A. Fonseca, *Diabetes Care*, 2009, **32**, S237–S245.

14 A. Liston and C. E. Whyte, *Immunol. Cell Biol.*, 2020, **98**, 349–350.

15 N. I. Hanafi, A. S. Mohamed, S. H. Sheikh Abdul Kadir and M. H. D. Othman, *Biomolecules*, 2018, **8**, 159.

16 Q. Qu, Y. Chen, Y. Wang, S. Long, W. Wang, H.-Y. Yang, M. Li, X. Tian, X. Wei, Y.-H. Liu, S. Xu, C. Zhang, M. Zhu, S. M. Lam, J. Wu, C. Yun, J. Chen, S. Xue, B. Zhang, Z.-Z. Zheng, H.-L. Piao, C. Jiang, H. Guo, G. Shui, X. Deng, C.-S. Zhang and S.-C. Lin, *Nature*, 2025, **643**, 192–200.

17 Q. Qu, Y. Chen, Y. Wang, W. Wang, S. Long, H.-Y. Yang, J. Wu, M. Li, X. Tian, X. Wei, Y.-H. Liu, S. Xu, J. Xiong, C. Yang, Z. Wu, X. Huang, C. Xie, Y. Wu, Z. Xu, C. Zhang, B. Zhang, J.-W. Feng, J. Chen, Y. Feng, H. Fang, L. Lin, Z. K. Xie, B. Sun, H. Tian, Y. Yu, H.-L. Piao, X.-S. Xie, X. Deng, C.-S. Zhang and S.-C. Lin, *Nature*, 2025, **643**, 201–209.

18 Y. Kim and K. O. Chang, *J. Virol.*, 2011, **85**, 12570–12577.

19 A. K. Schupp, M. Trilling, S. Rattay, V. T. K. Le-Trilling, K. Haselow, J. Stindt, A. Zimmermann, D. Häussinger, H. Hengel and D. Graf, *J. Virol.*, 2016, **90**, 6686–6698.

20 L. Luo, W. Han, J. Du, X. Yang, M. Duan, C. Xu, Z. Zeng, W. Chen and J. Chen, *Molecules*, 2018, **23**, 3315.

21 H. Yan, B. Peng, Y. Liu, G. Xu, W. He, B. Ren, Z. Jing, J. Sui and W. Li, *J. Virol.*, 2014, **88**, 3273–3284.

22 F. Kong, X. Niu, M. Liu and Q. Wang, *Vet. Microbiol.*, 2021, **257**, 109097.

23 A. Carino, F. Moraca, B. Fiorillo, S. Marchianò, V. Sepe, M. Biagioli, C. Finamore, S. Bozza, D. Francisci, E. Distrutti, B. Catalanotti, A. Zampella and S. Fiorucci, *Front. Chem.*, 2020, **8**, 572885.

24 T. Brevini, M. Maes, G. J. Webb, B. V. John, C. D. Fuchs, G. Buescher, L. Wang, C. Griffiths, M. L. Brown, W. E. Scott, 3rd, P. Pereyra-Gerber, W. T. H. Gelson, S. Brown, S. Dillon, D. Muraro, J. Sharp, M. Neary, H. Box, L. Tatham, J. Stewart, P. Curley, H. Pertinez, S. Forrest, P. Mlcochova, S. S. Varankar, M. Darvish-Damavandi, V. L. Mulcahy, R. E. Kuc, T. L. Williams, J. A. Heslop, D. Rossetti, O. C. Tysoe, V. Galanakis, M. Vila-Gonzalez, T. W. M. Crozier, J. Bargehr, S. Sinha, S. S. Upponi, C. Fear, L. Swift, K. Saeb-Parsy, S. E. Davies, A. Wester, H. Hagström, E. Melum, D. Clements, P. Humphreys, J. Herriott, E. Kijak, H. Cox, C. Bramwell, A. Valentijn, C. J. R. Illingworth, B. Dahman, D. R. Bastaich, R. D. Ferreira, T. Marjot, E. Barnes, A. M. Moon, A. S. T. Barritt, R. K. Gupta, S. Baker, A. P. Davenport, G. Corbett, V. G. Gorgoulis, S. J. A. Buczacki, J. H. Lee, N. J. Matheson, M. Trauner, A. J. Fisher, P. Gibbs, A. J. Butler, C. J. E. Watson, G. F. Mells, G. Dougan, A. Owen, A. W. Lohse, L. Vallier and F. Sampaziotis, *Nature*, 2023, **615**, 134–142.

25 S. Fiorucci, G. Urbani, M. Biagioli, V. Sepe, E. Distrutti and A. Zampella, *Biochem. Pharmacol.*, 2024, **228**, 115983.

26 Anglo-Saxon remedy kills hospital superbug MRSA, <https://www.newscientist.com/article/dn27263-anglo-saxon-remedy-kills-hospital-superbug-mrsa/#.VRo-zuEqHQ>, accessed October 14, 2025.

27 F. Harrison, A. E. L. Roberts, R. Gabrilska, K. P. Rumbaugh, C. Lee and S. P. Diggle, *mBio*, 2015, **6**, e01129.

28 C. Lin, Y. Wang, M. Le, K.-F. Chen and Y.-G. Jia, *Bioconjugate Chem.*, 2021, **32**, 395–410.

29 S. Mishra and S. Patel, *Med. Chem.*, 2020, **16**, 385–391.

30 P. G. do Nascimento, T. L. Lemos, M. C. Almeida, J. M. de Souza, A. M. Bizerra, G. M. Santiago, J. G. da Costa and H. D. Coutinho, *Steroids*, 2015, **104**, 8–15.

31 J. Wu, T. T. Yu, R. Kuppusamy, M. M. Hassan, A. Alghalayini, C. G. Cranfield, M. D. P. Willcox, D. S. Black and N. Kumar, *Int. J. Mol. Sci.*, 2022, **23**, 4623.

32 S. Kumar, J. Thakur, K. Yadav, M. Mitra, S. Pal, A. Ray, S. Gupta, N. Medatwal, R. Gupta, D. Mishra, P. Rani, S. Padhi, P. Sharma, A. Kapil, A. Srivastava, U. D. Priyakumar, U. Dasgupta, L. Thukral and A. Bajaj, *ACS Biomater. Sci. Eng.*, 2019, **5**, 4764–4775.

33 K. Yadav, P. S. Yavvari, S. Pal, S. Kumar, D. Mishra, S. Gupta, M. Mitra, V. Soni, N. Khare, P. Sharma, C. V. Srikanth, A. Kapil, A. Singh, V. K. Nandicoori and A. Bajaj, *Bioconjugate Chem.*, 2019, **30**, 721–732.

34 C. Saal, in *Solubility in Pharmaceutical Chemistry*, ed. S. S. Christoph and N. Anita, De Gruyter, Berlin, Boston, 2020, ch. 9, pp. 229–258.

35 D. Gupta, D. Bhatia, V. Dave, V. Sutariya and S. Varghese Gupta, *Molecules*, 2018, **23**, 1719.

36 M. C. Carey, *Hepatology*, 1984, **4**, 66s–71s.

37 A. Fini, A. Roda, R. Fugazza and B. Grigolo, *J. Solution Chem.*, 1985, **14**, 595–603.

38 P. C. Acharya, S. Marwein, B. Mishra, R. Ghosh, A. Vora and R. K. Tekade, in *Dosage Form Design Considerations*, ed. R. K. Tekade, Academic Press, 2018, vol. i, ch. 13, pp. 435–472.

39 F. M. S. Costa, A. Granja, R. L. Pérez, I. M. Warner, S. Reis, M. L. C. Passos and M. L. M. F. S. Saraiva, *Int. J. Mol. Sci.*, 2023, **24**, 15714.

40 F. M. S. Costa, M. L. M. F. S. Saraiva and M. L. C. Passos, *J. Mol. Liq.*, 2025, **417**, 126654.

41 D. D. Yang, N. Chutiwitoonchai, F. Wang, P. Tian, S. Sureram, X. Lei, C. Mahidol, S. Ruchirawat and P. Kittakoop, *Sci. Rep.*, 2025, **15**, 6380.

42 J. Pekala, B. Patkowska-Sokoł, R. Bodkowski, D. Jamroz, P. Nowakowski, S. Lochyński and T. Librowski, *Curr. Drug Metab.*, 2011, **12**, 667–678.



43 M. M. Adeva-Andany, I. Calvo-Castro, C. Fernández-Fernández, C. Donapetry-García and A. M. Pedre-Piñeiro, *IUBMB Life*, 2017, **69**, 578–594.

44 K. Kashani, M. H. Rosner and M. Ostermann, *Eur. J. Intern. Med.*, 2020, **72**, 9–14.

45 A. M. Wiedeman, S. I. Barr, T. J. Green, Z. Xu, S. M. Innis and D. D. Kitts, *Nutrients*, 2018, **10**, 1513.

46 S. H. Zeisel and K. A. da Costa, *Nutr. Rev.*, 2009, **67**, 615–623.

47 T. Thaweerattanasinp, A. Wanitchang, J. Saenboonrueng, K. Srisutthisamphan, N. Wanases, S. Sungsuwan, A. Jongkaewwattana and T. Chailangkarn, *PeerJ*, 2023, **11**, e14918.

48 S. Sureram, N. Chutiwittoonchai, T. Pooprasert, W. Sangsopha, S. Limjiasahapong, N. Jariyasopit, Y. Sirivatanauksorn, S. Khoomrung, C. Mahidol, S. Ruchirawat and P. Kittakoop, *Int. J. Biol. Macromol.*, 2024, **273**, 133059.

49 S. S. Bhawal, P. A. Hassan, S. L. Gawali, S. R. Patil, V. N. Patil, S. H. Solanki, D. L. Manyala and D. S. Varade, *J. Mol. Liq.*, 2022, **349**, 118193.

50 F. M. S. Costa, M. L. M. F. S. Saraiva and M. L. C. Passos, *J. Mol. Liq.*, 2022, **368**, 120750.

51 J. Gao, Y. Hu, S. Li, Y. Zhang and X. Chen, *Chem. Phys.*, 2013, **410**, 81–89.

52 E. Villalobos-Sánchez, J. M. Márquez-Villa, A. D. Vega-Rodríguez, D. A. Curiel-Pedraza, A. A. Canales-Aguirre, J. Bravo-Madrigal, J. C. Mateos-Díaz and D. E. Elizondo-Quiroga, *Viruses*, 2025, **17**, 416.

53 J.-H. Xing, T.-M. Niu, B.-S. Zou, G.-L. Yang, C.-W. Shi, Q.-S. Yan, M.-J. Sun, T. Yu, S.-M. Zhang, X.-Z. Feng, S.-H. Fan, H.-B. Huang, J.-H. Wang, M.-H. Li, Y.-L. Jiang, J.-Z. Wang, X. Cao, N. Wang, Y. Zeng, J.-T. Hu, D. Zhang, W.-S. Sun, W.-T. Yang and C.-F. Wang, *Microbiome*, 2024, **12**, 20.

54 Y.-Q. Zhang, B. Wang, Y.-L. Yang, J.-X. Meng, M.-D. Zhang, Y.-K. Li, B. Dong, Y. Zhang, B.-W. Liu, D. Yang, C.-M. Ji, Y.-W. Huang and S. J. Zhu, *iMeta*, 2025, e70061.

55 A. V. Petrova, I. E. Smirnova, S. V. Fedij, Y. N. Pavlyukova, V. V. Zarubaev, T. Tran Thi Phuong, K. Myint Myint and O. B. Kazakova, *Molbank*, 2023, **2023**, M1626.

56 F. Kong, X. Niu, M. Liu and Q. Wang, *Vet. Microbiol.*, 2021, **257**, 109097.

57 X. Liang, K. Liu, X. Jia, C. Cheng, M. Zhang, L. Kong, Q. Li, Z. Liu, M. Li, J. Li, Y. Wang and A. Xu, *Acta Pharm. Sin. B*, 2024, **14**, 3513–3527.

58 Q. Gao, Y. Xu, Y. Feng, X. Zheng, T. Gong, Q. Kuang, Q. Xiang, L. Gong and G. Zhang, *Int. J. Biol. Macromol.*, 2024, **266**, 130939.

59 P.-Y. Chen, C. Wang, Y. Zhang, C. Yuan, B. Yu, X.-G. Ke, H.-Z. Wu, Y.-F. Yang and X.-C. Xiao, *Nat. Prod. Commun.*, 2021, **16**, 1934578X211024032.

60 E. S. Winkler, S. Shrihari, B. L. Hykes, S. A. Handley, P. S. Andhey, Y.-J. S. Huang, A. Swain, L. Droit, K. K. Chebrolu, M. Mack, D. L. Vanlandingham, L. B. Thackray, M. Cella, M. Colonna, M. N. Artyomov, T. S. Stappenbeck and M. S. Diamond, *Cell*, 2020, **182**, 901–918.

61 Z. Xun, X. Yao, C. Lin, X. Yang, Y. Zhang, X. Yang, Y. He, R. Jiang, Y. Lan, Y. Ye, D. Ye, S. Chen, K. Ma, W. Wu, S. Xu, B. Yang, C. Liu, J. Chen, Q. Zheng and Q. Ou, *JHEP Rep.*, 2025, **7**, 101456.

62 T. Hu, J. Tong, Y. Yang, C. Yuan, J. Zhang and J. Wang, *Front. Med.*, 2025, **12**, 1494248.

63 Y. Yu, G. F. Li, J. Li, L. Y. Han, Z. L. Zhang, T. S. Liu, S. X. Jiao, Y. W. Qiao, N. Zhang, D. C. Zhan, S. Q. Tang and G. Yu, *Expert Rev. Anti-Infect. Ther.*, 2024, **22**, 1239–1250.

64 R. E. Costello, K. M. J. Waller, R. Smith, G. F. Mells, A. Y. S. Wong, A. Schultze, V. Mahalingasivam, E. Herrett, B. Zheng, L.-Y. Lin, B. MacKenna, A. Mehrkar, S. C. J. Bacon, B. Goldacre, L. A. Tomlinson, J. Tazare and C. T. Rentsch, The OpenSAFELY collaborative, the LH&W NCS (or Convalescence) Collaborative, *Commun. Med.*, 2024, **4**, 238.

65 C. He, M. Jiang, Q. Xiong and Z. Huang, *Sci. Rep.*, 2025, **15**, 5814.

66 T. H. Sannasiddappa, P. A. Lund and S. R. Clarke, *Front. Microbiol.*, 2017, **8**, 1581.

67 K.-J. Ma, Z. Li, R.-C. Bai, H.-J. Zhang, C. Zhang and L. Liu, *Cryst. Res. Technol.*, 2023, **58**, 2300218.

68 C.-C. Xie, Z.-L. Zhao, M.-Y. Huang, Z. Li, H.-J. Zhang and L. Liu, *Cryst. Growth Des.*, 2023, **23**, 6535–6547.

69 I. Nugrahani, A. F. Nuur Aini and M. S. Wibowo, *Heliyon*, 2024, **10**, e40373.

70 M. C. Jennings, L. E. Ator, T. J. Paniak, K. P. Minbile and W. M. Wuest, *Chembiochem*, 2014, **15**, 2211–2215.

71 M. T. García, E. Bautista, A. de la Fuente and L. Pérez, *Pharmaceutics*, 2023, **15**, 1806.

72 K. N. Ibsen, H. Ma, A. Banerjee, E. E. L. Tanner, S. Nangia and S. Mitragotri, *ACS Biomater. Sci. Eng.*, 2018, **4**, 2370–2379.

